



Discover Generics

Cost-Effective CT & MRI Contrast Agents

 FRESENIUS
KABI

[WATCH VIDEO](#)

AJNR

Early differential diagnosis of infantile neuronal ceroid lipofuscinosis, Rett syndrome, and Krabbe disease by CT and MR.

S L Vanhanen, R Raininko and P Santavuori

AJNR Am J Neuroradiol 1994, 15 (8) 1443-1453

<http://www.ajnr.org/content/15/8/1443>

This information is current as
of June 1, 2025.

Early Differential Diagnosis of Infantile Neuronal Ceroid Lipofuscinosis, Rett Syndrome, and Krabbe Disease by CT and MR

Sanna-Leena Vanhanen, Raili Raininko, and Pirkko Santavuori

PURPOSE: To compare early radiologic findings in three clinically similar progressive encephalopathies of childhood. **METHODS:** Brain CT and/or MR studies were done in 57 children 3 to 36 months of age: 16 with infantile neuronal ceroid lipofuscinosis, 5 with Rett syndrome, 6 with Krabbe disease, and 30 control subjects with normal neurologic status. In addition, previous descriptions in the literature were collected. **RESULTS:** No significant changes were seen in Rett syndrome. Early atrophy was found in infantile neuronal ceroid lipofuscinosis and in Krabbe disease, being more severe in the latter. The thalami were hyperdense in 4 of 13 patients with infantile neuronal ceroid lipofuscinosis and in 1 of 4 patients with Krabbe disease (in the literature in 12 of 30 examinations). Cerebral calcifications and density abnormalities in the cerebral and cerebellar white matter were seen in Krabbe disease only. On MR, the white matter changes in the two diseases were differently located. In every patient with infantile neuronal ceroid lipofuscinosis, decreased T2 signal was seen in the thalami and periventricular high-signal rims after the age of 13 months. Hypointensity of the thalami and basal ganglia was seen in both diseases, but Krabbe disease showed more variations. Abnormalities of cerebellar intensity were found in Krabbe disease only. **CONCLUSIONS:** CT and MR are of value in the differential diagnosis of these three diseases. MR especially facilitates the early diagnosis of infantile neuronal ceroid lipofuscinosis.

Index terms: Krabbe disease; Brain, diseases; Brain, computed tomography; Brain, magnetic resonance; Pediatric neuroradiology

AJNR Am J Neuroradiol 15:1443–1453, Sep 1994

Infantile neuronal ceroid lipofuscinosis, Rett syndrome, and Krabbe disease are progressive encephalopathies occurring throughout the world. In the early stages these diseases, although differing in underlying metabolic disorder and in course, have many clinical features in common. Until now the differential diagnosis based on clinical features has been difficult, especially between infantile neuronal ceroid lipo-

fuscinosis and Rett syndrome (1). The most common type of Krabbe disease is the infantile form, which differs from infantile neuronal ceroid lipofuscinosis and Rett syndrome in both time of onset and clinical findings, and so usually causes little diagnostic difficulty, although the differential diagnosis from the late-onset form of Krabbe disease may be difficult.

Early diagnoses of these diseases is important for counseling the affected families about future pregnancies. Both infantile neuronal ceroid lipofuscinosis and Krabbe disease are transmitted as autosomal recessive traits. Prenatal diagnosis, possible for the latter for many years, recently became available for infantile neuronal ceroid lipofuscinosis (2, 3).

In this report we present brain computed tomographic (CT) and magnetic resonance (MR) findings in infantile neuronal ceroid lipofuscinosis, Rett syndrome, and Krabbe disease. We also compare the results for our series with those of previous reports, to ascertain the value

Received August 5, 1993; accepted after revision January 4, 1994.

This study was supported by grants from the Arvo and Lea Ylppö Foundation and the Finnish Lions Club Association.

From the Department of Child Neurology, University of Helsinki (S.L.V., P.S.), and the Department of Radiology, University Central Hospital of Helsinki (R.R.), Finland.

Address reprint requests to Sanna-Leena Vanhanen, MD, Department of Child Neurology, Children's Hospital, University of Helsinki, SF-00290 Helsinki, Finland.

AJNR 15:1443–1453, Sep 1994 0195-6108/94/1508–1443
© American Society of Neuroradiology

of neuroradiologic examinations in the differential diagnosis of these three disorders.

Subjects and Methods

Subjects

Twenty-seven patients were examined: 16 with infantile neuronal ceroid lipofuscinosis, 5 with Rett syndrome, and 6 with Krabbe disease. The diagnosis of infantile neuronal ceroid lipofuscinosis was confirmed by electron microscopy in all cases. All the girls with Rett syndrome fulfilled the criteria for Rett syndrome (4). The diagnosis of Krabbe disease was confirmed by enzymatic tests. Radiologic examinations were performed at the ages of 3 to 36 months.

The control group consisted of 30 children of the same age. Of these children, 14 were referred for some nonspecific neurologic complaint such as a single seizure, headache, or dizziness; 16 children were followed up because of mothers' infectious diseases. The latter group had no clinical symptoms; serologic tests for infectious agents were negative; and their electroencephalograms were normal. The neurologic status of all the control subjects, examined by child neurologists, was normal. The radiologic examinations were made with the consent of the parents and the Ethics Committee.

Methods

CT of the brain was performed by the routine technique without contrast enhancement. Axial sections 4 to 5 mm thick were used in the posterior fossa and sections 8 to 10 mm thick in the remainder of the brain. MR images were obtained on a 1.0-T system. After a T1-weighted sagittal scout image set, axial sections 5 mm thick with gaps of 1 mm were used with the spin-echo sequences 500/20/2 (repetition time/echo time/excitations) and 2500/22 to 90/1; in children younger than 1 year of age repetition time was 3500 milliseconds in the latter image set. Additional sets of images, mostly T1-weighted sagittal images, were obtained for most of the subjects. Matrix size was 256 × 256, and field of view 230 mm. Contrast enhancement was not used.

CT and MR images were evaluated by two of the authors in a joint session. The degree of cerebral atrophy was evaluated from CT images as described in the literature (5, 6). The dimensions measured were the diameters of the frontal horns and bodies of the lateral ventricles, the third ventricles, the interhemispheric spaces, and the cerebral sulci. Measures of the lateral ventricles were related to the diameters of the intracranial spaces. The same criteria were used for MR images, if appropriate. Evaluation of sulcal size in the upper sections and in the cerebella was based largely on the MR experience of the authors. The images of the control subjects were evaluated first, to test the validity of the criteria of normality. Then the images of the patients were evaluated in arbitrary order without clinical information. The readers could not be absolutely blinded, because some of the children had been examined

earlier in the same institution, and their grossly pathologic images were recognizable.

Altogether, 27 examinations were performed in infantile neuronal ceroid lipofuscinosis: 9 patients underwent both CT and MR; 4 patients underwent CT only; and 3 patients MR only. One child was examined three times with MR, at 3, 13, and 19 months of age. He was followed up primarily because of congenital toxoplasmosis confirmed by serologic tests. His psychomotor development and electroencephalogram were normal, but he had slight left-sided muscular hypertonia. The first symptoms of infantile neuronal ceroid lipofuscinosis became apparent at 15 months. Nine radiologic examinations were performed in Rett syndrome: 1 patient underwent CT only; and 4 patients underwent both examinations. In addition, 1 girl had a follow-up CT at 5 years of age. Nine examinations were performed in Krabbe disease: 4 patients with the infantile form underwent CT only; 1 patient underwent MR only; and the only patient with the late-onset form underwent both CT and MR twice. The control group underwent MR only, to avoid ionizing irradiation.

The maximum occipitofrontal circumference was measured with a metal tape in every child from birth every 2 to 4 months during the first year of life and about once a year after that. These values were available during the entire follow-up time, because head size is monitored in all children until the age of 7 years in our country.

Results

The results obtained with the two methods are combined in Tables 1, 2, and 3.

Control Subjects

Atrophic Changes. Head size was normal (on the 50th percentile). Two children examined at 3 to 4 months of age had prominent ambient cisterns. Otherwise, the control subjects fulfilled all the criteria of normality.

Density Changes on CT. No changes were detected in the brain parenchyma.

Intensity Changes on T2-weighted Images. MR images fulfilled the criteria of normality (7, 8). Maturation progressed according to normal milestones (7). Between the ages of 13 and 15 months the basal ganglia appeared isointense with the white matter, attaining hyperintensity with respect to the adjacent white matter between the ages of 16 and 22 months, after which the brain had the adult appearance.

Infantile Neuronal Ceroid Lipofuscinosis

Atrophic Changes. The head size of the 3-month-old child was normal; from the age of

TABLE 1: Atrophic changes seen in infantile neuronal ceroid lipofuscinosis, Krabbe disease, and Rett syndrome during the first 3 years of life

Age, mo	Infantile Neuronal Ceroid Lipofuscinosis		Krabbe Disease		Rett Syndrome		Control Subjects	
	Cerebrum	Brain Stem, Cerebellum	Cerebrum	Brain Stem, Cerebellum	Cerebrum	Brain Stem, Cerebellum	Cerebrum	Brain Stem, Cerebellum
0-12	1/2	2/2	Infantile	3/4	2/4		0/9	2/9
13-18	9/9	2/9	Infantile	1/1	1/1		0/12	0/12
			Late-onset	0/1	0/1			
19-24	12/12	5/12	Late-onset	0/1	0/1	0/2	0/2	0/3
25-36	4/4	2/4	Late-onset	0/2	0/2	2/7	0/7	0/6
Total	26/27	11/27	Infantile	4/5	3/5	2/9	0/9	0/30
			Late-onset	0/4	0/4			2/30

Note.—Number of examinations with atrophic changes/total number of examinations are given.

12 months all the patients were microcephalic (head circumference on the 10th percentile or below it). Atrophy (the cerebrospinal fluid-containing spaces were too large in relation to the size of the intracranial space) was seen from the age of 12 months onward and generalized atrophy from the age of 20 months (Figs 1-3). The severity of the atrophy was variable. Cerebral atrophy was more severe than cerebellar atrophy. The cerebral sulci and the third ventricles were enlarged most frequently, in 26 of 27 and in 25 of 27 examinations, respectively. Enlarged cerebellar sulci and/or dilatation of the fourth ventricles were seen in 9 of 27 examina-

tions. In one 26-month-old patient the heads of the caudate nuclei were markedly reduced in size. Callosal atrophy was a constant finding from the age of 13 months. The calvaria were thickened in patients older than 2 years of age.

Density Changes on CT. The thalami were hyperdense to the basal ganglia (Fig 1) in 4 of 13 patients between the ages of 16 and 23 months, but the hyperdensity was distinct in only 1 patient. No white matter changes were seen.

Intensity Changes on T2-weighted Images. The brain looked normal at the age of 3 months

TABLE 2: Abnormal attenuation on CT

Infantile Neuronal Ceroid Lipofuscinosis		Krabbe Disease		Rett Syndrome
		Infantile Form	Late-onset Form	
No. of patients	13	4	1	5
No. of examinations	13	4	2	5
Abnormal	4	3	2	
Age (mo) and abnormality	16	7	17	
	Slightly hyperdense thalami	Slightly hyperdense thalami	Calcifications in the thalami and putamina	
		Hypodensity in the left frontal white matter		
		Increased density difference between cerebellar white and gray matter		
	17	8	26	
	Hyperdense thalami	Calcified foci in the centra semiovale and at the lateral margins of the basal ganglia	Calcifications in the putamina and in the right thalamus	
	18	10		
	Slightly hyperdense thalami	Suspect hypodensity of the white matter		
		Increased density difference between cerebellar white and gray matter		
	23			
	Slightly hyperdense thalami			

TABLE 3: Abnormal intensity relationships between the brain structures in infantile neuronal ceroid lipofuscinosis, Krabbe disease, and Rett syndrome on T2-weighted MR images

Infantile Neuronal Ceroid Lipofuscinosis		Krabbe Disease		Rett Syndrome
		Infantile Form	Late-onset Form	
No. of patients	12	1	7	4
No. of examinations	14	1	2	4
Abnormal	13	1	2	0
Age (mo) and abnormality	13–26	16	19 and 31	
	Strong hypointensity of thalami to central white matter and to basal ganglia (13/13)	Hyperintense foci in the thalami (1/1)	Putamina isointense to the white matter and hyperintense to the other basal ganglia and thalami (2/2)	
	Periventricular high-signal rims (13/13)	Strong hyperintensity of white matter around the trigoni and posterior bodies of the lateral ventricles (1/1)	Whole cerebral white matter hyperintense to cortical gray matter; especially high intensity in central area (2/2)	
	17–26	Corpus callosum hyperintense to central white matter, small hyperintense foci in the internal capsules (1/1)		
	Basal ganglia hypointense to central white matter (8/11)			
	Larger deep white matter hyperintensity (2/11)			
	19–26			
	Peripheral cerebral white matter hyperintense to cortical gray matter (9/9)			

Note.—Numbers of examinations with abnormal intensities/total numbers of examinations are given in parentheses.

in the examination performed for toxoplasmosis. The most striking and permanent findings in infantile neuronal ceroid lipofuscinosis were strong thalamic hypointensity with respect to the white matter and the basal ganglia and thin high-signal rims around the entire lateral ventricles, except in the temporal lobes, from the age of 13 months onward (Figs 2 and 3). Hyperintensities posterior to the trigoni, normally noticed on T2-weighted images from the age of approximately 15 months onward (8), were extremely strong in nine patients, being of the intensity of the cerebrospinal fluid. The deep white matter, except for the periventricular high-signal rims, remained hypointense to the peripheral white matter in all except two patients, aged 17 and 24 months. The increased intensity of the peripheral white matter in relation to the cortical gray matter became distinct at the age of 19 months (Fig 3B). The maturation of the subcortical white matter of the precentral gyrus progressed normally until the age of 16 months. In three patients, this area still remained hypointense to the other (abnormal) areas of the peripheral white mat-

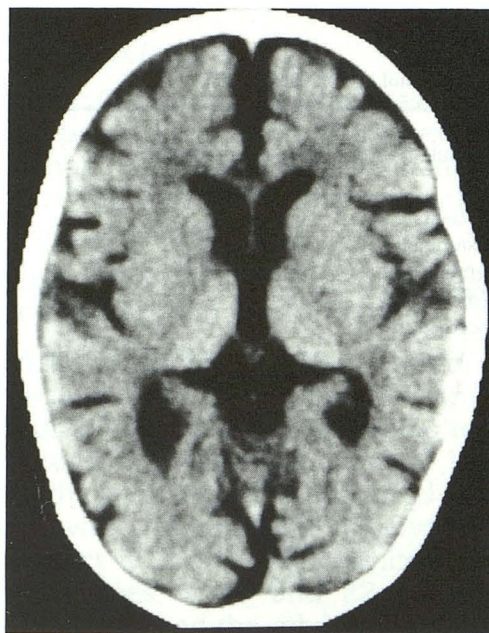


Fig 1. Infantile neuronal ceroid lipofuscinosis, 16-month-old girl. CT shows a dilated third ventricle and enlarged cerebral sulci. Sizes of the lateral ventricles are still within normal limits. The thalami are slightly hyperdense to the basal ganglia, and the white matter looks normal.

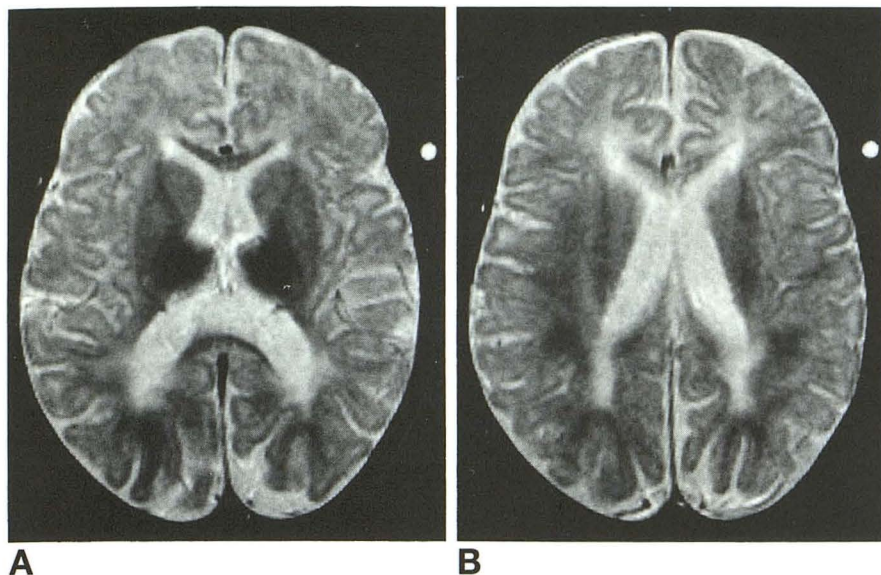


Fig 2. Infantile neuronal ceroid lipofuscinosis, 13-month-old girl, T2-weighted spin-echo (2500/90) MR images. Sulci and the third ventricle are slightly enlarged. Corpus callosum is thin (A). Thalamic hypointensity is striking. Periventricular high-signal rims are well seen (A and B). Peripheral white matter is more hyperintense to the cortical gray matter than in healthy children at this age.

ter at the ages of 23 to 26 months. In five patients this region did not differ from the adjacent pathologic areas after the age of 17 months; in four other patients some foci of normal lower intensity were detected. The basal ganglia were all of equal intensity and were hypointense to the adjacent white matter from the age of 17 months onward, which is the reverse of normal development (Fig 3A). However, the basal ganglia always had a higher signal intensity than the thalami. The corpus callosum retained normal intensity in every patient, despite the loss of volume. No distinct abnormality of intensity was seen in the cerebellum.

Rett Syndrome

Atrophic Changes. The head sizes of these girls were either normal or abnormally small (on the 50th percentile or below the 10th percentile). Slightly enlarged cerebral sulci were noted in two of nine examinations (head size was normal), and one of these two also showed slight dilatation of the third ventricle. The girl followed up from the age of 22 months showed some enlarged sulci only at 5 years.

Density Changes on CT. No pathologic attenuation was detected in the brain parenchyma.

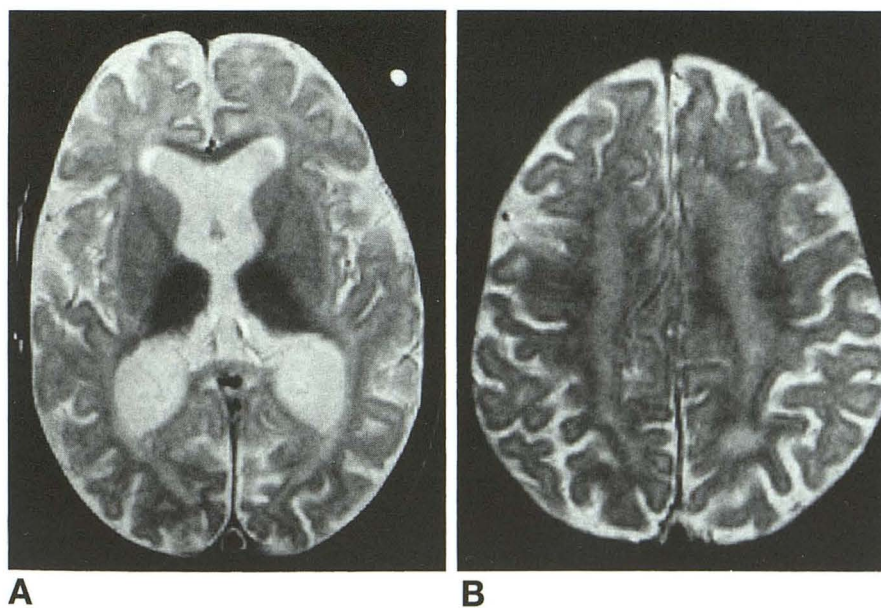


Fig 3. Infantile neuronal ceroid lipofuscinosis, 19-month-old boy with severe generalized atrophy. T2-weighted spin-echo (2500/90) MR images show decreased T2 signal of the thalami and high-signal rims around the ventricles (A and B). The basal ganglia look hypointense to white matter. The signal intensity of the peripheral white matter and cortical gray matter is reverse to normal.

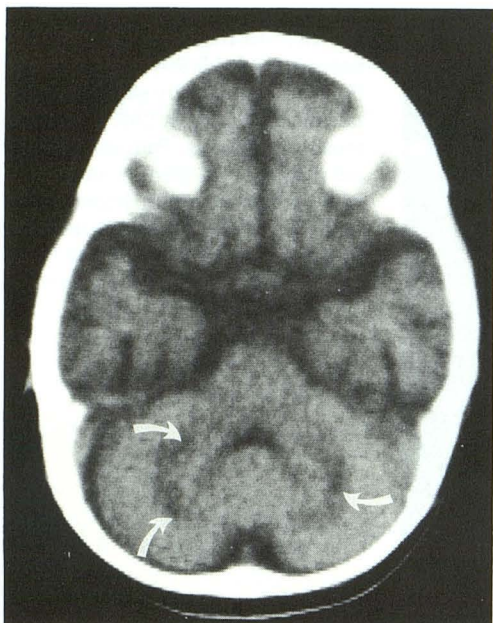


Fig 4. Infantile form of Krabbe disease, 10-month-old girl. CT shows increased density difference between central cerebellar white and gray matter. The difference between the pons and central cerebellar white matter is also abnormally high. Areas with lowest density are marked with arrows.

Intensity Changes on MR. There were no significant intensity changes.

Krabbe Disease

Atrophic Changes. All the children with the infantile form were microcephalic (below the 10th percentile). Cerebral atrophy was evident

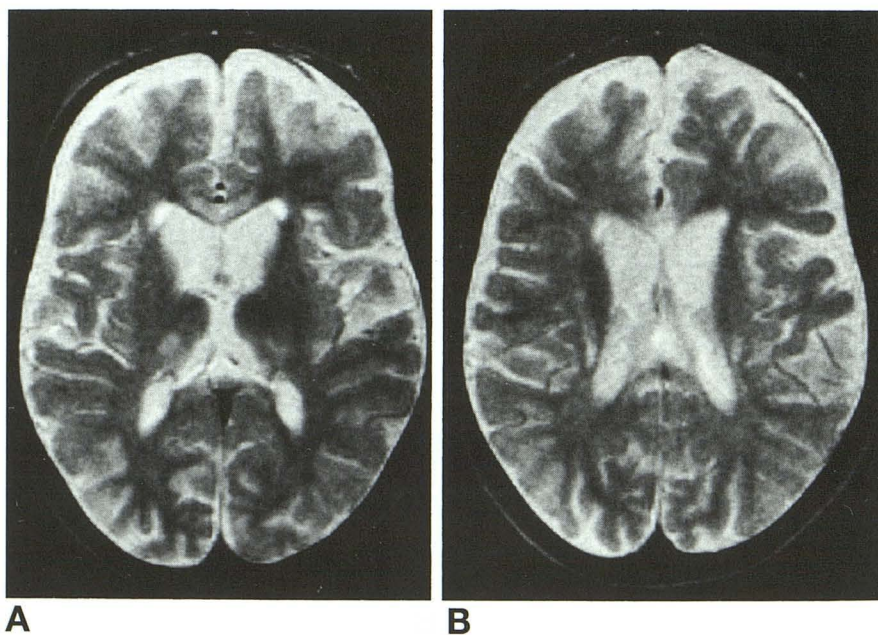
even at the age of 7 months and became severe at 10 months (Figs 4 and 5). The enlargement of the third ventricle was most severe. Cerebellar atrophy was not seen, but two of five examinations showed slightly enlarged ambient cisterns. In the only patient examined with MR, the heads of the caudate nuclei (Fig 5A) and the mesencephalon were reduced in size at the age of 16 months. The head size of the only child with the late-onset form was small (below the second percentile from the age of 15 months). She had no atrophy on CT at the ages of 17 (Fig 6) or 26 months, but MR, first performed at the age of 19 months, revealed callosal atrophy.

Density Changes on CT. Slight thalamic hyperdensity was seen in one of four patients and calcified foci in the cerebral white matter in one of four patients with the infantile form; two of four patients had obvious or probable cerebral and cerebellar white matter hypodensity. All the children with the infantile form had undergone CT before the age of 12 months.

In the only child with the late-onset form, calcifications were seen in the thalami and putamina from the age of 17 months (Fig 6). No white matter changes were revealed.

Intensity Changes on T2-weighted Images. In the infantile form, abnormal high signal intensity was noted in the white matter around the trigoni and posterior bodies of the lateral ventricles at the age of 16 months (Fig 5B). High signal intensity was also observed in the corpus

Fig 5. Infantile form of Krabbe disease, 16-month-old girl with severe generalized atrophy, T2-weighted spin-echo (2500/90) MR images. The signal intensity of the white matter is increased around the trigoni and the posterior bodies of the lateral ventricles (B). The corpus callosum is also of high signal intensity (A and B). High-signal foci are shown in the lateral posterior nuclei of the thalami (A).



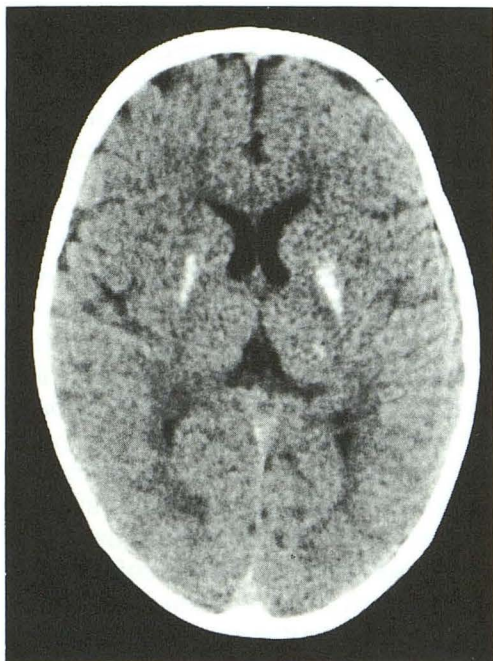


Fig 6. Late-onset form of Krabbe disease, 17-month-old girl. CT shows calcifications in both putamina and in the left thalamus.

callosum and focally in the anterior limbs of the internal capsules. The lateral posterior nuclei of the thalami showed high signal intensity (Fig 5A). No distinct abnormality of intensity was seen in the cerebellum.

In this case of the late-onset form the entire white matter was hyperintense to the cortical gray matter on T2-weighted images at the age of 19 months; the intensity was highest in the

central area (Fig 7). The difference in intensity between the central and peripheral areas seemed to be less at 31 months than at 19 months. The thalami were hypointense to the adjacent white matter. The basal ganglia showed variable intensities (Table 3 and Fig 7A). There was no abnormality of intensity in the cerebellum.

Discussion

The group of diseases known as neuronal ceroid lipofuscinoses is one of the most common progressive encephalopathies (9, 10). The diagnosis of the infantile type (infantile neuronal ceroid lipofuscinosis) has been based on neurophysiologic and ophthalmologic findings at around 20 to 30 months of age (10, 11) and is confirmed by electron microscopy of a rectal biopsy specimen, which reveals cytoplasmic inclusions with their typical finely granular structures (12). The diagnosis of Rett syndrome, which affects girls only, is based on clinical criteria (4). The basic pathogenesis is not yet known for either disorder. Krabbe disease (globoid cell leukodystrophy) is caused by deficiency of the enzyme lysosomal hydrolase galactocerebroside β -galactosidase (β -galactocerebroside), and the diagnosis can be confirmed by enzymatic methods. Infantile neuronal ceroid lipofuscinosis and Rett syndrome present with very similar manifestations in the very first stages of disease. The rapid regression

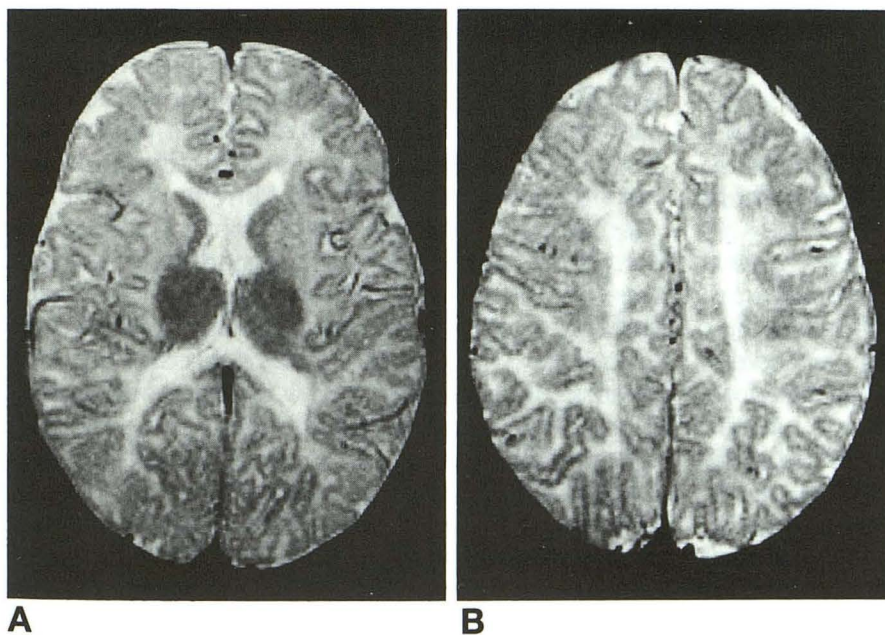


Fig 7. Late-onset form of Krabbe disease, same patient as in Figure 6 at the age of 19 months, T2-weighted spin-echo (2500/90) MR images. The entire white matter is of abnormal high signal intensity, the central area being more pathologic than the periphery. The thalami and caudate nuclei are of similar intensity, but they both are hypointense to the putamina and white matter.

at 1 to 2 years of age with loss of acquired fine motor skills, learned words, and ability to communicate, and also the successively developing hand and finger stereotypies are found in both diseases. Deceleration of head growth occurs earlier in infantile neuronal ceroid lipofuscinosis, and visual failure is a typical finding in this disease. The infantile form of Krabbe disease is characterized by marked irritability and fluctuating muscle tone appearing within 3 to 6 months of birth, followed within a few weeks by opisthotonus posturing, visual failure, loss of tendon reflexes, hypertonic fits, intermittent fevers, and feeding problems. Further psychomotor development ceases, and death occurs 1 to 3 years later. The late-onset form of Krabbe disease occurs less commonly and is more difficult to diagnose, because it is clinically more heterogeneous and usually progresses more slowly. Clinical manifestations appear between ages 2 (sometimes earlier) and 6 years and include visual failure, cerebellar ataxia, spastic hemiparesis, peripheral neuropathy, and dementia. The course of infantile neuronal ceroid lipofuscinosis, and occasionally of the late-onset form of Krabbe disease (13), is extremely rapid around 2 years of age.

CT is useful in the early diagnosis of both forms of Krabbe disease, although in the late-onset form it still may be normal at the age of 8 years (14), often revealing high-density areas in typical locations in the thalami and basal ganglia. Opinions differ about the origin of hyperdensities on CT. The hyperdensity may be related to deposition of galactocerebroside and to astrogliosis (15). Thalamic hyperdensity is more frequent and distinct than in infantile neuronal ceroid lipofuscinosis. It also has been found in patients with GM₂ gangliosidosis (16) and sometimes in Alexander disease (17), but the time of onset and clinical picture are helpful in differential diagnosis.

The symmetric, punctate high-density areas may represent calcification after demyelination (18). Histologic characteristics of Krabbe disease do not include calcifications; however, they may have been present in regions not prepared as histologic specimens. Feanny et al (19) reported periventricular calcifications, which were confirmed at autopsy in one patient with the infantile form of Krabbe disease. Calcifications, typically situated in the thalami, basal ganglia, or corona radiata, have been found in the infantile form in 10 of 34 examinations (15,

18–22; our cases). Few CT reports (six patients) on the late-onset form of Krabbe disease are available before the age of 3 years (23–27); our patient is the seventh. Typical calcifications have been found in two to five of eight examinations in the late-onset form (23, 25, 27; our patient), in some publications the descriptions are lacking in clarity. Cerebral calcifications also have been described in Cockayne disease (28), mitochondrial encephalopathies (29), Alexander disease (17, 30), Fahr syndrome (31), tuberous sclerosis, and some infections, but these diseases all differ from Krabbe disease in history or clinical symptoms. A typical CT finding in the leukodystrophies is hypodensity of the cerebral white matter, but this is relatively less marked in Krabbe disease than in the other leukodystrophies (32). In the infantile form of Krabbe disease it may be seen from the age of 5 months (15, 33), and in the late-onset form it is seen in some patients after 15 months of age (23, 24). In the infantile form of Krabbe disease hyperdense areas appear earlier than the extensive hypodensity of the deep cerebral and cerebellar white matter (15, 20, 34); in the late-onset form of Krabbe disease it is not known which CT abnormality appears first.

An increased density difference between the cerebellar white matter and gray matter has been seen from the age of 5 months in some patients with the infantile form of Krabbe disease. We found it in two of three patients.

MR is more sensitive than CT in demonstrating abnormalities in metabolic diseases. In infantile neuronal ceroid lipofuscinosis the development of the central nervous system looked normal during the first months of life. It is noteworthy that pathologic findings were detected at the age of 13 months in a child who did not yet have clinical symptoms of infantile neuronal ceroid lipofuscinosis. It is not known at what age the intensity changes and atrophy appeared, but MR of the same child revealed no abnormalities at the age of 3 months. In most cases deceleration of head growth begins before the appearance of clinical signs of the disease (10; the present study), and now we have shown that there also may be MR findings of the disease before any symptoms are manifested. Strong thalamic hypointensity with respect to the white matter and to the basal ganglia and thin periventricular high-signal rims from 13 months onward were typical early findings on T2-weighted images. It is interesting that the same

kinds of periventricular high-signal rims have been detected in older children in another neuronal ceroid lipofuscinosis disease, variant Jansky-Bielschowsky disease (variant late-infantile neuronal ceroid lipofuscinosis) (35). The periventricular signal intensity may be relatively high in some healthy children, and it may be enhanced with some sequences, but the difference between healthy children and those with infantile neuronal ceroid lipofuscinosis is obvious when images obtained by the same technique are compared. In most cases the deep white matter, except the periventricular high-T2 signal areas, still remained hypointense to the peripheral white matter (Table 3), but the peripheral white matter became hyperintense to the cortical gray matter, indicating a pathologic process in these areas of the cerebral white matter.

A few brain biopsy results are available (36). One 20-month-old patient with infantile neuronal ceroid lipofuscinosis showed neuronal storage, incipient loss of cortical neurons, and gliosis. Most of the axons and myelin sheaths seemed to be preserved; however, the number of astrocytes was increased, indicating incipient tissue destruction. In contrast, histologic examinations of autopsy specimens from patients 9 to 10 years old showed almost complete loss of cortical neurons, as well as of axons and myelin sheaths in the white matter (37). Loss of myelin thus seems to be caused by wallerian degeneration.

According to our findings, which are consistent with these neuropathologic observations, myelination seems to start normally in infantile neuronal ceroid lipofuscinosis but begins to deviate by the age of 19 months. MR images are compatible with myelin degradation. Wallerian degeneration (38) and increased white matter interstitial fluid may account for the increased white matter intensity. The subcortical white matter under the precentral gyrus remained hypointense to the subcortical white matter, at least focally, in other locations; this may be because of spared white matter islands. This is in agreement with histologic studies, which showed that the giant Betz cells in the precentral gyrus and the myelinated fibers in the white matter were preserved longer under the precentral gyri than elsewhere (37).

The decrease in basal ganglionic and thalamic signals on T2-weighted images is generally thought to be caused by increased deposi-

tion of iron (39, 40), this being perhaps a nonspecific response to degeneration and decreased neurotransmitter synthesis. The accumulation of iron may be associated with the intracellular storage of lipofuscin in the nerve cells in neuronal ceroid lipofuscinosis disorders (41, 42). However, other investigators (43, 44) have not found such a concentration of iron in ceroid or lipofuscin. Lipofuscin does not significantly or specifically affect T2 relaxivity (39). No histologic reports were available concerning the thalami or basal ganglia of young patients with infantile neuronal ceroid lipofuscinosis (younger than 3 years of age).

In the infantile form of Krabbe disease cerebral, and often also cerebellar, intensity changes on T2-weighted images combined with evident cerebral atrophy appear early during the first year of life (18, 21, 22, 45-48; the present study). In the late-onset form, atrophy may be absent (14). In both forms, white matter involvement usually begins from the parietal periventricular area then extends in all directions, but on T2-weighted images the site of the primary abnormality may vary. Thus the radiologic distinction between the leukodystrophies is not clear. Abnormal intensities are noticed early in the corpus callosum and internal capsules on T2-weighted images. These structures were not involved in infantile neuronal ceroid lipofuscinosis. Another difference between these two diseases is that abnormalities of cerebellar intensity on T2-weighted images are not seen in patients with infantile neuronal ceroid lipofuscinosis in these age groups. In the previous reports concerning Krabbe disease, cerebellar hyperintensities were seen in most of the patients with the infantile form (66%) (18, 22, 45, 47). They have not been found in the late-onset form, but reports of this form are few. We did not find these changes in either form of the disease. In both forms of Krabbe disease, the thalami and basal ganglia look hypointense to the adjacent white matter, but there may be foci with higher signal intensities, or one of these structures may differ from the others. In all leukodystrophies decreased T2 signal intensity is seen in the thalami and basal ganglia (34, 49, 50), and the thalami may have lower signal intensities. Solely thalamic hypointensity has been described in GM₂ gangliosidosis (16). However, these diseases differ clinically from Krabbe disease and infantile neuronal ceroid lipofuscinosis, and the evaluation of white mat-

ter involvement facilitates the diagnosis. At least 150 girls with Rett syndrome, examined by some neuroradiologic methods, have been described in the literature (51–58) (Witt-Engerström I, Rett Syndrome: The Late Infantile Regression Period, dissertation, University of Göteborg, Göteborg, Sweden, 1990). The great majority of these patients have been older than ours. A small percentage have had mild to moderate diffuse sulcal enlargement, especially in the frontal area (57). In patients 5 to 25 years of age global cerebral hypoplasia, progressive cerebellar atrophy increasing with age, and hypoplasia of the corpus callosum have been found (58). We observed mild cerebral atrophy in two of nine examinations. Atrophy seemed not to progress markedly during the first few years of the disease. No changes in signal intensity have been described in Rett syndrome, but most of the reports including MR have been very superficial and seem to be based mainly on T1-weighted images. In our four patients, we did not find abnormalities in signal intensity with any of the sequences used.

Conclusions

Radiologic diagnosis of infantile neuronal ceroid lipofuscinosis can be made when the following criteria are fulfilled on MR: decreased T2 signal in the thalami, high-signal rims in the periventricular white matter, and variable cerebral atrophy, although the atrophy of the corpus callosum is constant. Cerebellar atrophy is less obvious. The basal ganglia are hypointense to the adjacent white matter from the age of 17 months, and the peripheral cerebral white matter is hyperintense to the cortex from the age of 19 months on T2-weighted images.

Krabbe disease can be diagnosed in a relatively specific way by MR and CT. White matter hyperintensities, usually beginning in the parietal periventricular areas, are seen on T2-weighted images during the first year of life in the infantile type and after the age of 16 to 17 months in the late-onset type. Extension into the splenium and internal capsules is common, and in most cases the cerebellar white matter is involved. The thalami and basal ganglia show variable intensities on T2-weighted images. Early cerebral atrophy is typical of the infantile, but not of the late-onset, type. CT is diagnostically valuable in demonstrating parenchymal, mostly cerebral, calcifications or diffuse hyper-

density of the thalami or basal ganglia in about 55% of the patients.

The majority of patients with Rett syndrome have no radiologic abnormalities, and the rest have only slight nonspecific atrophy. However, the absence of radiologic abnormalities is of value to the clinician in differential diagnostic problems.

Thus, MR, perhaps supplemented with CT if Krabbe disease is suspected, is a helpful tool in the clinical diagnosis of these three disorders, and it facilitates the early diagnosis of infantile neuronal ceroid lipofuscinosis in particular.

Acknowledgments

We thank Dr Leena Valanne, Dr Anna-Liisa Saukkonen, and Dr Raija Lappalainen for contributing MR images.

References

1. Hagberg B, Witt-Engerström I. Early stages of the Rett syndrome and infantile neuronal ceroid lipofuscinosis: a differential diagnosis. *Brain Dev* 1990;12:20–22
2. Rapola J, Salonen R, Ämmälä P, Santavuori P. Prenatal diagnosis of the infantile type of neuronal ceroid lipofuscinosis by electron microscopic investigation of human chorionic villi. *Prenat Diagn* 1990;10:553–559
3. Järvelä I, Schleutker J, Haataja L, et al. Infantile neuronal ceroid lipofuscinosis (INCL, CLN1) maps to the short arm of chromosome 1. *Genomics* 1991;8:170–173
4. The Rett Syndrome Diagnostic Criteria Work Group. Diagnostic criteria for Rett syndrome. *Ann Neurol* 1988;23:425–428
5. Meese W, Kluge W, Grumme T, Hopfenmüller W. CT evaluation of the CSF spaces of healthy persons. *Neuroradiology* 1980;19:131–136
6. Gyldensted C. Measurements of the normal ventricular system and hemispheric sulci of 100 adults with computed tomography. *Neuroradiology* 1977;14:183–192
7. Barkovich AJ. Normal brain development. In: Atlas SW, ed. *Magnetic Resonance Imaging of the Brain and Spine*. New York: Raven Press, 1991:129–142
8. Braffman BH, Trojanowski JQ, Atlas SW. The aging brain and neurodegenerative disorders. In: Atlas SW, ed. *Magnetic Resonance Imaging of the Brain and Spine*. New York: Raven Press, 1991:567–618
9. Rider JA, Rider DL. Batten disease: past, present and future. *Am J Med Genet* 1988;Suppl 5:21–26
10. Santavuori P. Neuronal ceroid-lipofuscinoses in childhood. *Brain Dev* 1988;10:80–83
11. Santavuori P, Järvelä I, Haltia M, et al. Update on infantile neuronal ceroid-lipofuscinosis (INCL). *Brain Dev* 1990;12:661
12. Rapola J, Santavuori P, Savilahti E. Suction biopsy of rectal mucosa in the diagnosis of infantile and juvenile types of neuronal ceroid-lipofuscinoses. *Hum Pathol* 1984;15:352–360
13. Lyon G, Hagberg B, Evrard PH, Allaire C, Pavone L, Vanier M. Symptomatology of late onset Krabbe's leukodystrophy: the European experience. *Dev Neurosci* 1991;13:240–244
14. Phelps M, Aicardi J, Vanier M-T. Late onset Krabbe's leukodystrophy: a report of four cases. *J Neurol Neurosurg Psychiatry* 1991;54:293–296

15. Cavanagh N, Kendall B. High density on computed tomography in infantile Krabbe's disease: a case report. *Dev Med Child Neurol* 1986;28:799-802
16. Brismar J, Brismar G, Coates R, Gascon G, Ozand P. Increased density of the thalamus on CT scans in patients with GM2 gangliosidosis. *AJNR Am J Neuroradiol* 1990;11:125-130
17. Valk J, van der Knaap MS. Alexander's disease. In: *Magnetic Resonance of Myelin, Myelination, and Myelin Disorders*. Berlin: Springer-Verlag, 1989:165-172
18. Sasaki M, Sakuragawa N, Takashima S, Hanaoka S, Arima M. MRI and CT findings in Krabbe disease. *Pediatr Neurol* 1991;7:283-288
19. Feanny SJ, Chuang SH, Becker LE, Clarke JTR. Intracerebral paraventricular hyperdensities: a new CT sign in Krabbe globoid cell leukodystrophy. *J Inherited Metab Dis* 1987;10:24-27
20. Kwan E, Drace J, Enzman D. Specific CT findings in Krabbe disease. *AJNR Am J Neuroradiol* 1984;5:453-458
21. Mirowitz SA, Sartor K, Prensky AJ, Gado M, Hodges FJ. Neurodegenerative diseases of childhood: MR and CT evaluation. *J Comput Assist Tomogr* 1991;15:210-222
22. Baram TZ, Goldman AM, Percy AK. Krabbe disease: specific MRI and CT findings. *Neurology* 1986;36:111-115
23. Kurokawa T, Chen Y-J, Nagata M, Hasuo K, Kobayashi T, Kitaguchi T. Late infantile Krabbe leukodystrophy: MRI and evoked potentials in a Japanese girl. *Neuropediatrics* 1987;18:182-183
24. Fiumara A, Pavone L, Siciliano L, Tinè A, Parano E, Innico G. Late-onset globoid cell leukodystrophy: report on seven new patients. *Childs Nerv Syst* 1990;6:194-197
25. Epstein MA, Zimmerman RA, Rorke LB, Sladky JT. Late-onset globoid cell leukodystrophy mimicking an infiltrating glioma. *Pediatr Radiol* 1991;21:131-132
26. Kolodny EH, Raghavan S, Krivit W. Late-onset Krabbe disease (globoid cell leukodystrophy): clinical and biochemical features of 15 cases. *Dev Neurosci* 1991;13:232-239
27. Jardim L, Giugliani R, Fensom AH. Thalamic and basal ganglia hyperdensities: a CT marker for globoid cell leukodystrophy? *Neuropediatrics* 1992;23:30-31
28. Valk J, van der Knaap MS. Cockayne's disease. In: *Magnetic Resonance of Myelin, Myelination, and Myelin Disorders*. Berlin: Springer-Verlag, 1989:149-154
29. Valk J, van der Knaap MS. Mitochondrial leukoencephalopathy. In: *Magnetic Resonance of Myelin, Myelination, and Myelin Disorders*. Berlin: Springer-Verlag, 1989:130-136
30. Holland IM, Kendall BE. Computed tomography in Alexander's disease. *Neuroradiology* 1980;20:103-106
31. Billard C, Dulac O, Bouloche J, et al. Encephalopathy with calcifications of the basal ganglia in children: a reappraisal of Fahr's syndrome with respect to 14 new cases. *Neuropediatrics* 1989;20:12-19
32. Ieshima A, Eda I, Matsui A, Yoshino K, Takashima S, Takeshita K. Computed tomography in Krabbe's disease: comparison with neuropathology. *Neuroradiology* 1983;25:323-327
33. Barnes DM, Enzmann DR. The evolution of white matter disease as seen on computed tomography. *Radiology* 1981;138:379-383
34. Hatten HP Jr. Dysmyelinating leukodystrophies: "LACK proper myelin." *Pediatr Radiol* 1991;21:477-482
35. Autti T, Raininko R, Launes J, Nuutila A, Santavuori P. Brain findings in variant Jansky-Bielschowsky disease on CT, MRI and SPECT. *Pediatr Neurol* 1992;8:121-126
36. Haltia M, Rapola J, Santavuori P, Keränen A. Infantile type of so-called neuronal ceroid lipofuscinosis, 2: morphological and biochemical studies. *J Neurol Sci* 1973;18:269-285
37. Haltia M, Rapola J, Santavuori P. Infantile type of so-called neuronal ceroid-lipofuscinosis: histological and electron microscopic studies. *Acta Neuropathol (Berl)* 1973;26:157-170
38. Kuhn MJ, Johnson KA, Davis KR. Wallerian degeneration: evaluation with MR imaging. *Radiology* 1988;168:199-202
39. Drayer B, Burger P, Darwin R, Riederer S, Herfkens R, Johnson GA. Magnetic resonance imaging of brain iron. *AJNR Am J Neuroradiol* 1986;7:373-380
40. Drayer B. Imaging of the aging brain. *Radiology* 1988;166:785-796
41. Zeman W, Donohue S, Dyken P, Green J. The neuronal ceroid-lipofuscinoses (Batten-Vogt syndrome). In: Vinken P, Bruyn GW, eds. *Handbook of Clinical Neurology*. vol X. Amsterdam: North Holland Publishing, 1970:588-679
42. Vistnes AL, Henriksen T, Nicolaissen B, Armstrong D. Free radicals and aging. Electron spin resonance studies on neuronal lipopigments of cells grown in vitro. *Mech Ageing Dev* 1983;22:335-339
43. Johansson E, Lindh E, Alanen T, et al. Elemental profiles in certain neurological disorders. *Med Biol* 1984;62:139-142
44. Heiskala H, Gutteridge JMC, Westermarck T, Alanen T, Santavuori P. Bleomycin-detectable iron and phenanthroline-detectable copper in the cerebrospinal fluid of patients with neuronal ceroid-lipofuscinoses. *Am J Med Genet* 1988; (suppl 5):193-202
45. Winants D, Bernard C, Galloy MA, Hoeffel JC, Vidailhet M. Scanographie et IRM de la maladie de Krabbe. *J Radiol* 1988;69:697-700
46. Nowell MA, Grossman RI, Hackney DB, Zimmerman RA, Goldberg HI, Bilaniuk LT. MR imaging of white matter disease in children. *AJNR Am J Neuroradiol* 1988;9:503-509
47. Farley TJ, Ketonen LM, Bodensteiner JB, Wang DD. Serial MRI CT findings in infantile Krabbe disease. *Pediatr Neurol* 1992;8:455-458
48. Yamanouchi H, Kasai H, Sakuragawa N, Kurokawa T. Palatal myoclonus in Krabbe disease. *Brain Dev* 1991;13:355-358
49. Demaerel P, Faubert C, Wilms G, Casaer P, Piepgras U, Baert AL. MR findings in leukodystrophy. *Neuroradiology* 1991;33:368-371
50. van der Knaap MS, Valk J. The reflection of histology in MR imaging of Pelizaeus-Merzbacher disease. *AJNR Am J Neuroradiol* 1989;10:99-103
51. Zoghbi HY, Percy AK, Glaze DG, Butler IJ, Riccardi VM. Reduction of biogenic amine levels in the Rett syndrome. *N Engl J Med* 1985;313:921-924
52. Budden S. Rett syndrome: studies of 13 affected girls. *Am J Med Genet* 1986;24 (suppl):99-109
53. Naidu S, Murphy M, Moser HW, Rett A. Rett syndrome: natural history in 70 cases. *Am J Med Genet* 1986;24 (suppl):61-72
54. Xi-Ru W, Dong-Hong Z, Qing L, Ding-Fang B, Chi-Hua Z. Rett syndrome in China: report of 19 patients. *Pediatr Neurol* 1988;4:126-127
55. Krägeloh-Mann I, Schroth G, Niemann G, Michaelis R. The Rett syndrome: magnetic resonance imaging and clinical findings in four girls. *Brain Dev* 1989;11:175-178
56. Naidu S, Hyman S, Piazza K, et al. The Rett syndrome: progress report on studies at the Kennedy Institute. *Brain Dev* 1990;12:5-7
57. Nihei K, Naitoh H. Cranial computed tomographic and magnetic resonance imaging studies on the Rett syndrome. *Brain Dev* 1990;12:101-105
58. Murakami JW, Courchesne E, Haas RH, Press GA, Yeung-Courchesne R. Cerebellar and cerebral abnormalities in Rett syndrome. *AJR Am J Roentgenol* 1992;159:177-183